High-power quantum-dot superluminescent tapered diode under CW operation

Research Article | Vol. 27, No. 8 | 15 Apr 2019 | OPTICS EXPRESS 10981
Optics EXPRESS

High-power quantum-dot superluminescent tapered diode under CW operation

ADAM F. FORREST,[1,4,*] MICHEL KRAKOWSKI,[2] PAOLO BARDELLA,[3] AND MARIA ANA CATALUNA[1,4]

[1]*Institute of Photonics and Quantum Sciences, School of Engineering and Physical Sciences, Heriot-Watt University, Edinburgh Campus, Edinburgh EH14 4AS, UK*
[2]*III-V Lab, 1 Avenue Augustin Fresnel, Campus de Polytechnique, 91767 Palaiseau, France*
[3]*Dipartmento di Elettronica e Telecomunicazioni, Politecnico di Torino, I-10129 Turin, Italy*
[4]*Previously also with the School of Engineering, Physics and Mathematics, University of Dundee, Dundee DD1 4HN, UK*
[*]*adam.forrest@hw.ac.uk*

Abstract: A high-power quantum-dot superluminescent diode is demonstrated under continuous-wave operation, with an output power of 137.5 mW and a corresponding spectral bandwidth of 21 nm. This represents not only the highest output power, but also a record-high power spectral density of 6.5 mW/nm for a CW-operated superluminescent diode in the 1.1 - 1.3 μm spectral region, marking more than a 6-fold increase with respect to the state of the art. The two-section contact layout of the reported device introduces additional degrees of freedom, which enable a wide tunability of the bandwidth and power depending on the desired application. A maximum bandwidth of 79 nm was recorded, with an output power of 1.4 mW. The high-power continuous-wave operation of this device would be particularly relevant for continuous, high-speed, high-sensitivity spectroscopy, imaging and sensing applications, as well as in optical communications.

1. Introduction

Superluminescent diodes (SLDs) are fundamental light components in a wide range of applications such as in optical coherence tomography [1], fiber gyroscopes [2], optical spectroscopy [3], optical communications [4], and random number generation [5].

High power and high spectral density are particularly important for spectroscopy and other sensing applications which require a moderate spectral bandwidth. This is also of relevance whenever there is a requirement for high-speed sensing, as higher power sources can significantly speed up acquisition times to achieve a required signal-to-noise-ratio, thus enabling the capture of events at faster rates. For example, this is the case of incoherent broadband cavity enhanced absorption spectroscopy, whereby the use of a broadband source allows for the simultaneous chemical analysis of a variety of components [6]. For this purpose, arc-lamps and light-emitting diodes are the sources typically used. However, low spectral densities and low spatial coherence mean that practical levels of sensitivity can only be achieved at the expense of long acquisition times. Recently, it was demonstrated that SLDs are practical sources for such applications [3], whereby their high spatial coherence and spectral power density (200 μW/nm, in this case [3]) were shown to enable high-sensitivity chemical analysis with a moderate acquisition time. More recently, a supercontinuum source tailored for such applications has been demonstrated with a high spectral density of 5 mW/nm [7]. While supercontinuum sources typically have high spectral power density, their significantly higher cost, footprint and complexity are impediments to wider field deployment.

#358589 https://doi.org/10.1364/OE.27.010981
Journal © 2019 Received 25 Jan 2019; revised 22 Mar 2019; accepted 22 Mar 2019; published 4 Apr 2019

Optics EXPRESS

A high power spectral density is also of importance in the context of other applications where the output is spectrally sliced, such as wavelength division multiplexing [4,8] and random number generation (in which the use of SLDs was recently demonstrated) [5]. A range of approaches can be pursued in order to optimize SLDs' performance. For example, increasing the device length is a common approach to boost the output power [9], as long as the threshold for laser emission is not reached. The use of tapered device configurations, particularly the combination of SLD and a tapered semiconductor optical amplifier have shown promising output power levels in the 1.1 – 1.3 μm spectral region, up to around 500 mW, albeit under pulsed pumping conditions [10–12]. Under CW pumping conditions, the maximum optical power achieved in the 1.1 - 1.3 μm spectral band was 107 mW [13].

Indeed, a common approach to access a high output peak power of SLDs is to use a pulsed pumping regime with a low duty cycle. This allows extremely high driving currents to be applied for short periods of time without inducing damage and, if the pulse is short enough, can reduce thermal effects which detriment the output power and cause spectral narrowing [14]. However, pulsed pumping does not allow for continuous sensing applications and requires more complicated driving circuitry for the source and sensors compared to simple continuous-wave approaches. Importantly, the signal-to-noise ratio in sensing/spectroscopy applications is also enhanced with continuous operation.

The spectral region below 1.1 μm is easily accessed by GaAs-based quantum-well structures. Likewise, emission wavelengths immediately above 1.3 μm are readily obtained from InP-based quantum-well structures. However, access to the band between 1.1 – 1.3 μm presents challenges, opening a unique opportunity for quantum-dot materials to provide the basis of devices emitting in this waveband. In the spectral region between 1.1 – 1.3 μm, quantum-dot (QD) materials have shown great promise, particularly by using chirped QD layers, whereby the average size of the QDs can be engineered in each layer in order to target a particular emission wavelength [15]. This approach has led to the broadest optical spectrum emission, of around 240 nm, in continuously driven QD-based SLDs in this spectral region (1.1 – 1.3 μm) [16] as well as supported the development of broadly-tunable QD lasers [17,18].

In this paper, we present a novel chirped QD SLD with a two-section, tapered waveguide, emitting at a wavelength around 1235 nm that demonstrated a record-high output power (137.5 mW) and average power spectral density (6.5 mW/nm) for a CW operated SLD in the 1.1 – 1.3 μm wavelength range.

2. SLD design and fabrication

The layout of the QD SLD used in this work is outlined schematically in Fig. 1(a). The chirped QD wafer was grown by Innolume GmbH (Germany) on a heavily silicon-doped n-type GaAs substrate by molecular beam epitaxy. Electrical and optical confinement were enabled by $Al_{0.35}Ga_{0.65}As$ cladding layers. The active region contained ten layers of InAs quantum dots, each capped by $In_{0.15}Ga_{0.85}As$ and separated by 33 nm GaAs barriers. A group of three QD layers were engineered for a target emission wavelength at 1211 nm, followed by another group of three layers at 1243 nm and finally a group of four layers engineered to emit at 1285 nm (listed in order from the p-doped to the n-doped side). In order to achieve this, the thickness of the $In_{0.15}Ga_{0.85}As$ capping layer was different for each group of QD layers. This is a common growth technique, whereby the average size of the quantum dots within each QD layer is proportional to the thickness of the capping layer, thus resulting in a shift of their emission wavelength [19]. This QD wafer structure is identical to the one previously used in the demonstration of a high-power tunable laser [17].

#358589 https://doi.org/10.1364/OE.27.010981
Journal © 2019 Received 25 Jan 2019; revised 22 Mar 2019; accepted 22 Mar 2019; published 4 Apr 2019

Optics EXPRESS

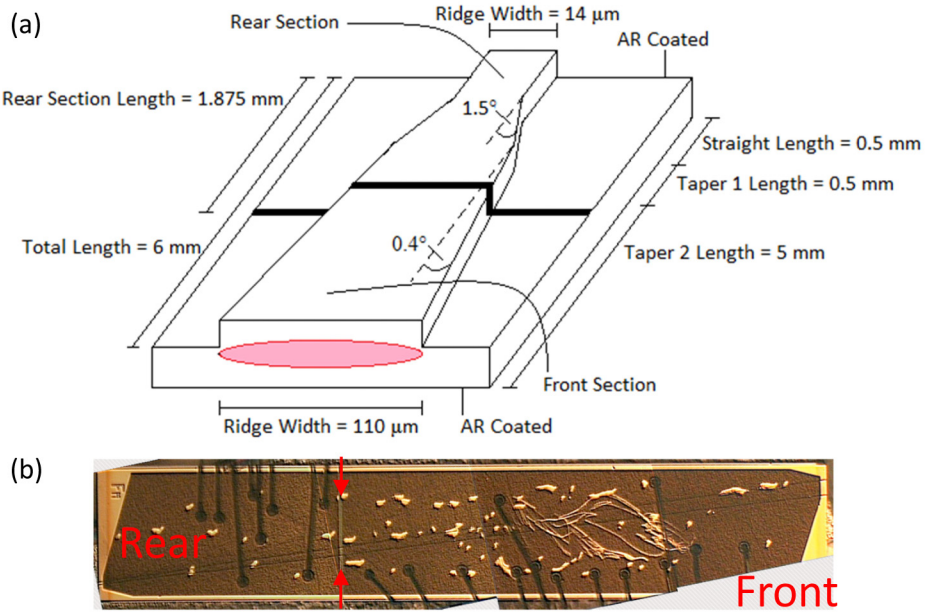

Fig. 1. (a). Superluminescent diode design schematic (not to scale). The SLD's tilt angle (7°) is not represented, for simplicity. (b). Top-down photo of SLD. The isolation trench is indicated in the photo by the red arrows.

The wafer was subsequently processed by III-V Lab (France) into a two-section, tapered SLD (Fig. 1). The device had a total length of 6 mm and consisted of three distinct geometrical segments. At the rear of the device was a short, straight segment with a length of 0.5 mm and a ridge width of 14 µm. Following on from this was the first of two tapered segments which had a length of 0.5 mm and a taper angle of 1.5°. The final segment had a smaller taper angle of 0.4° that ran along the remaining 5 mm of the device length resulting in a front facet width of 110 µm.

This unique waveguide design was derived based on simulations similar to those performed in [20], with the goal of simultaneously enhancing both the gain and beam quality emitted from the tapered facet through the manipulation of the waveguide geometry. In addition to this, and while the waveguide was firstly defined by proton bombardment via gain guiding, a weak index guiding ($\Delta n = 10^{-4}$) was also introduced through the shallow etching of the waveguide. This design feature increased the optical confinement and helped to mitigate the antiguiding effects associated with the proton bombardment [20].

The SLD's length was relatively long in order to boost the output power [9]. An isolation trench was etched into the contact layer 1.875 mm from the rear facet to create two electrically isolated sections. The location of the trench meant that the rear contact serviced the straight, first tapered and part of the second tapered segments while the front contact pumped the remainder of the second tapered segment of the waveguide. The rationale for using a multi-section tapered design was to provide a further degree of freedom in the pumping conditions of the device, enhancing the tunability of the power and spectral characteristics [21].

An anti-reflection coating was deposited on both facets and the waveguide was tilted by an angle of 7° with respect to these – in order to prevent laser emission. The device was mounted p-side up on a copper heat sink and was maintained at a constant temperature of 20°C by a Peltier cooler and temperature controller. Both sections of the SLD were continuously pumped by separate constant current source diode drivers.

#358589 https://doi.org/10.1364/OE.27.010981
Journal © 2019 Received 25 Jan 2019; revised 22 Mar 2019; accepted 22 Mar 2019; published 4 Apr 2019

Optics EXPRESS

3. SLD performance

Measurements of the average power were made in free space using a broadband thermal power sensor (Thorlabs S302C) after the output of the SLD had been collimated using a combination of an aspheric and cylindrical lens. A broadband optical isolator was placed immediately after the collimation optics, i.e. before the power meter, to prevent any unwanted reflections disrupting the operation of the SLD. Measurements of the optical spectra were made through an optical fiber using an optical spectrum analyzer (Yokogawa AQ6370), again with an optical isolator in place.

The light-current characteristics of the SLD are shown in Fig. 2, depicting the average output power emitted from the front facet as a function of the front section current, at various fixed rear section currents. From these plots, the common SLD trend of superlinearly increasing output power with increasing front section driving current can be seen across the full range of rear section currents.

At rear section currents between 0.1 A and 0.6 A, a clear rollover in the output power can be seen as the front section current approached 5 A, limiting the maximum output power. The superluminescent region was limited by the onset of laser emission, at the highest current levels (above 4A, for a rear section of 0.7A). In fact, it can be observed that beyond this point, the light-current characteristic also departs from the trend exhibited by the other curves at different rear section currents.

In Table 1, the power, spectral bandwidth and average power spectral density of the SLD detailed in this work is compared to a selection of state-of-the-art CW operated devices emitting in the 1.1 – 1.3 μm spectral band that have been previously reported. The devices included in Table 1 were chosen from a vast number of reports [1,9,13,16,22–51] and mark some of the best reported bandwidth, average power or power spectral density for CW devices in the 1.1 – 1.3 μm waveband.

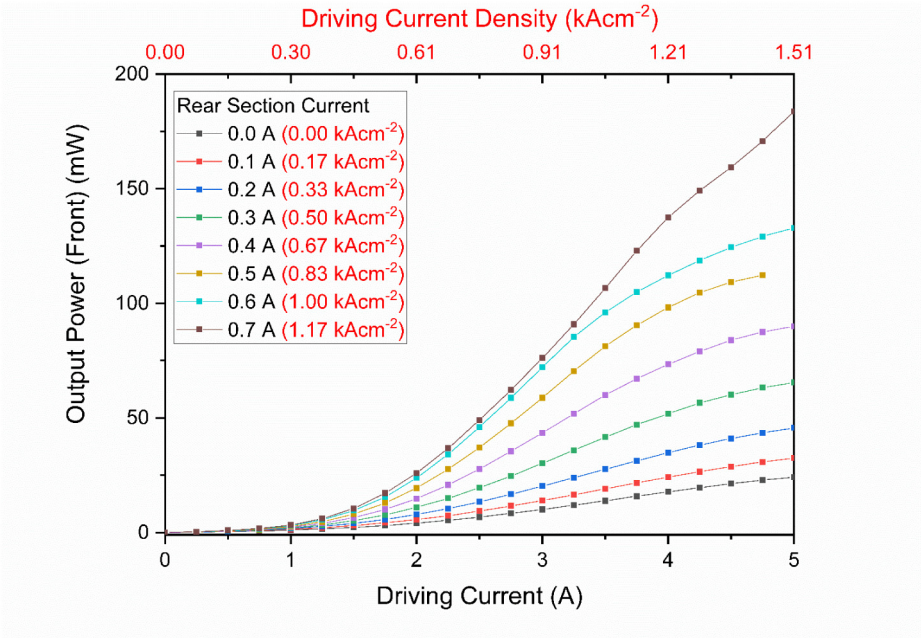

Fig. 2. Superluminescent diode output optical power vs front section driving current at various fixed rear section currents.

#358589 https://doi.org/10.1364/OE.27.010981

Received 25 Jan 2019; revised 22 Mar 2019; accepted 22 Mar 2019; published 4 Apr 2019

Optics EXPRESS

Table 1. Comparison of the spectral bandwidth (Δλ), average power (P_{avg}) and average power spectral density ($P_{avg}/\Delta\lambda$) of the device reported here to state of the art CW SLDs with a central wavelength (λ_c) between 1.1 – 1.3 µm selected from the literature [1,9,13,16,22–51].

λ_C (nm)	Δλ (nm)	P_{avg} (mW)	$P_{avg}/\Delta\lambda$ (mW/nm)	Reference
1120	178.8	1.30	0.01	[50]
1150	66.6	30.00	0.45	[51]
1154	148.0	0.13	<0.01	[23]
1170	112.0	107.0.	0.96	[13]
1235	**21.0**	**137.50**	**6.55**	**This Work**
1255	**79.0**	**1.40**	**0.02**	**This Work**
1258	142.0	0.30	<0.01	[33]
1260	85.0	35.00	0.41	[34]
1300	50.0	50.00	1.00	[9]
1300	200.0	10.00	0.05	[42]

The maximum power that was observed from our device in the superluminescent regime was 137.5 mW, the highest for a CW-biased device in the 1.1 - 1.3 µm spectral band, as highlighted in Table 1. This impressive output power was likely the result of both the tapered design and considerable length of the SLD waveguide, both of which have been shown to boost SLD output power [9,52]. Considering that the bandwidth of the optical spectrum at this power level was 21.3 nm, this corresponded to an average power spectral density of 6.5 mW/nm, more than 6 times the current state of the art for any CW SLD in the 1.1 – 1.3 µm wavelength range [9].

However, there is a clear trade-off between spectral bandwidth and optical power, as previously reported in the literature [9]. As shown in Fig. 3, it was possible to achieve a broader spectral bandwidth of 79 nm, albeit with less than 2 mW output power. This plot also highlights the flexibility afforded by the independent biasing of two electrical sections, which enables the selection of different regimes of operation with an emphasis on power or bandwidth, depending on the target application at hand.

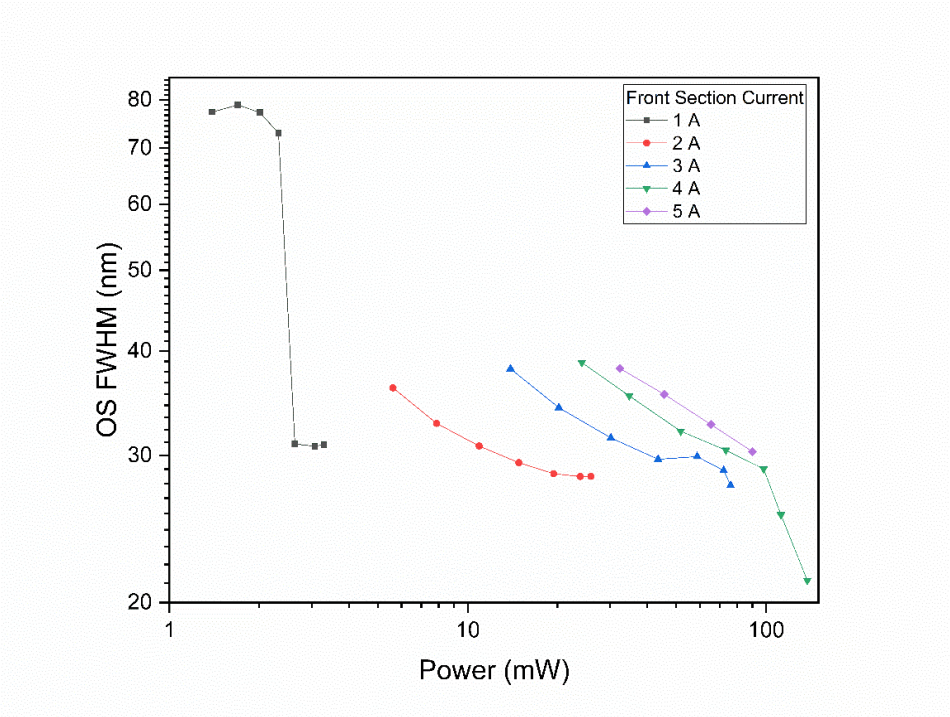

Fig. 3. Superluminescent diode optical spectrum (OS) FWHM spectral bandwidth vs output power at various front section driving currents.

#358589 https://doi.org/10.1364/OE.27.010981
Journal © 2019 Received 25 Jan 2019; revised 22 Mar 2019; accepted 22 Mar 2019; published 4 Apr 2019

Optics EXPRESS

Looking into the optical spectra in more detail, Fig. 4. shows spectra emitted from the SLD through a cross section of the range of front and rear section currents that were tested. Figure 4(a) shows the spectra at a fixed rear section current of 0.2 A where the largest bandwidth of 79 nm was observed (at 1 A front section current) and Fig. 4(b). shows optical spectra at a fixed front section current of 4 A where the largest power of 137.5 mW was observed (at a rear section current of 0.7 A). These plots clearly indicate that there was a strong dependence of the shape of the optical spectra on the biasing conditions of the SLD.

At 1 A of front section current, across the entire range of tested rear section currents, the optical spectra had a distinct double hump shape with two peaks centered at approximately 1235 nm and 1290 nm. The presence of the 1290 nm peak in these spectra indicated that there was a significant contribution from the ground state of the 1285 nm QD layers in the active region along with a composite contribution from the 1211 nm and 1243 nm layers to form the 1235 nm peak.

A similar trend in the spectral shape was also observed for increasing front section current above 1 A across the entire range of fixed rear section currents. As front section current was increased, the 1235 nm peak was seen to increase in power relative to the 1290 nm peak, particularly drastically between 1 A and 2 A of front section current, as the spectra transitioned to a single peak at 1235 nm.

The tendency for the optical spectra to adopt a single peak shape centered around 1235 nm despite the largest population of QDs within the active region being designed to emit at 1285 nm was likely the result of several factors. Firstly, it has been shown experimentally in QW structures [53,54] and through simulations in QD structures [55] that the carrier density in active region layers decreases as the distance from the p-side of the device increases. This is a result of the reduced mobility of holes compared to electrons and their preferential capture in QDs near the p-side compared to electrons near the n-side. In the chirped QD active region presented in this work, such an inhomogeneous carrier density would result in the longest wavelength QDs, which were furthest from the p-side of the device, having the lowest ground state population and hence making a diminished contribution to the optical spectrum.

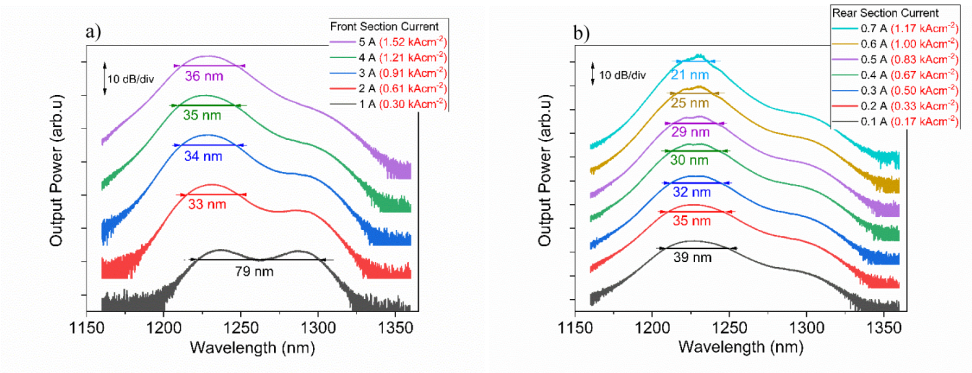

Fig. 4. Superluminescent diode optical spectra under various biasing conditions. (a) optical spectra at various front section driving currents at a fixed rear section current of 0.2 A. (b) optical spectra at various rear section currents at a fixed front section current of 4 A.

#358589 https://doi.org/10.1364/OE.27.010981
Journal © 2019 Received 25 Jan 2019; revised 22 Mar 2019; accepted 22 Mar 2019; published 4 Apr 2019

Optics EXPRESS

Continuation of this analysis implies that the highest carrier density was delivered to the three layers of quantum dots designed to emit at 1211 nm. However, the resultant optical spectra tended towards the much longer central wavelength of 1235 nm with increasing front and rear section current. A factor that could have resulted in this shift in the center wavelength towards the emission wavelength of the central three QD layers within the active region is the overlap of the transverse optical mode with the active region. Assuming that the transverse optical mode within the SLD waveguide is close to a fundamental Gaussian mode then the maximum optical intensity would overlap with roughly the center of the active region. This has the effect of boosting the amplification by the 1243 nm QD layers and hence shifts the spectrum towards wavelengths longer than 1211 nm.

The presence of the 1290 nm peak at low driving currents was likely the result of a state filling effect whereby the ground states of the larger QDs were filled more easily than the higher energy states of the smaller QDs within the active region. This effect has been observed before in QD SLDs where the optical spectrum was seen to broaden exclusively on the blue side as driving current was increased [56]. At low levels of current, where there is still significant thermal redistribution of carriers from shorter to longer wavelength QDs, this effect could have had a stronger influence than that of inhomogeneous carrier density within the active region.

All of the aforementioned dynamics which could have influenced the spectral shape along with thermal effects and the spectral response of the anti-reflective facet coating ultimately determined the achievable spectral bandwidth and also point to several ways in which SLD performance could be improved. For example, improvement in the bandwidth of the SLD could potentially be achieved through re-ordering of the chirped QD layers' position relative to the p-contact to reduce inhomogeneous current density. For example, instead of stacking three different groups of QD layers next to each other (three layers emitting at 1211 nm, followed by three at 1243 nm and then four at 1285 nm), different QD layers could be interleaved throughout the active region (1211 nm, 1243 nm, 1285 nm, 1211 nm, …). Alternatively, the size of the various QD layers could be carefully engineered so that the spectral gap between the ground and excited state of one layer of dots is filled-in by the ground state of a separate layer [27]. Further improvements in both power and spectral bandwidth could also be achieved by mounting the device p-side down with a bespoke submount, as enhanced thermal management has been shown to be valuable in boosting both optical power and spectral bandwidth [13].

4. Conclusions

A high-power tapered superluminescent diode with a chirped quantum-dot active region has been demonstrated, operating under CW driving conditions. A maximum output power of 137.5 mW was observed with a corresponding spectral bandwidth of 21.3 nm centered at 1235 nm. This represents a record-high value of output power from a CW-driven SLD in the spectral region between 1.1 – 1.3 μm and also corresponds to the highest average power spectral density (6.55 mW/nm) from a CW SLD in the same spectral region. Such power spectral density values are on a par with supercontinuum sources developed for spectroscopy applications. The lower cost and footprint of SLDs compared with supercontinuum sources means that this performance offers significant potential for high-speed, high-sensitivity sensing applications, as well as the ability to be used in portable systems for in situ measurements.

The multi-section electrical layout enabled a versatile range of combinations of optical power and spectral bandwidth, which can match particular target application needs. Indeed, while power levels of the order of 100 mW were regularly observed with typical spectral bandwidth values of around 30 nm, a maximum bandwidth of 79 nm was also recorded (albeit at a low output power of 1.4 mW).

#358589 https://doi.org/10.1364/OE.27.010981
Journal © 2019 Received 25 Jan 2019; revised 22 Mar 2019; accepted 22 Mar 2019; published 4 Apr 2019

Optics EXPRESS

Funding

H2020 European Research Council (ERC) (640537); FP7 Information and Communication Technologies (224338); Engineering and Physical Sciences Research Council/Biotechnology and Biological Sciences Research Council (EPSRC/BBSRC) PhD DTA studentship.

Acknowledgments

The authors would like to thank Innolume GmbH (Germany) for the growth of the QD wafers. The authors would like to thank T. Xu, M. Rossetti and I. Montrosset for stimulating discussions and Stephanie E. White for the photo in Fig. 1(b). From III-V Lab the authors would also like to thank M. Tran for SLD processing, Y. Robert for the SLD low-reflectivity coating, E. Vinet and M. Garcia for SLD mounting and M. Ruiz for characterization. Supporting data is available at https://doi.org/10.17861/92eba9c2-1a37-4bb6-a43a-d1a4a847f2e6.

References

1. P. D. L. Greenwood, D. T. D. Childs, K. Kennedy, K. M. Groom, M. Hugues, M. Hopkinson, R. A. Hogg, N. Krstajić, L. E. Smith, S. J. Matcher, M. Bonesi, S. MacNeil, and R. Smallwood, "Quantum dot superluminescent diodes for optical coherence tomography: device engineering," IEEE J. Sel. Top. Quantum Electron. **16**(4), 1015–1022 (2010).
2. R. Bergh, H. Lefevre, and H. Shaw, "An overview of fiber-optic gyroscopes," J. Lightwave Technol. **2**(2), 91–107 (1984).
3. W. Denzer, M. L. Hamilton, G. Hancock, M. Islam, C. E. Langley, R. Peverall, and G. A. D. Ritchie, "Near-infrared broad-band cavity enhanced absorption spectroscopy using a superluminescent light emitting diode," Analyst (Lond.) **134**(11), 2220–2223 (2009).
4. K.-Y. Liou and G. Raybon, "Operation of an LED with a single-mode semiconductor amplifier as a broad-band 1.3-μm transmitter source," IEEE Photonics Technol. Lett. **7**(9), 1025–1027 (1995).
5. X. Li, A. B. Cohen, T. E. Murphy, and R. Roy, "Scalable parallel physical random number generator based on a superluminescent LED," Opt. Lett. **36**(6), 1020–1022 (2011).
6. K. C. Cossel, E. M. Waxman, I. A. Finneran, G. A. Blake, J. Ye, and N. R. Newbury, "Gas-phase broadband spectroscopy using active sources: progress, status, and applications," J. Opt. Soc. Am. B **34**(1), 104–129 (2017).
7. A. Aalto, G. Genty, T. Laurila, and J. Toivonen, "Incoherent broadband cavity enhanced absorption spectroscopy using supercontinuum and superluminescent diode sources," Opt. Express **23**(19), 25225–25234 (2015).
8. D. K. Jung, S. K. Shin, C.-H. Lee, and Y. C. Chung, "Wavelength-division-multiplexed passive optical network based on spectrum-slicing techniques," IEEE Photonics Technol. Lett. **10**(9), 1334–1336 (1998).
9. M. Sugo, Y. Shibata, H. Kamioka, Y. Tohmori, and M. Yamamoto, "High-power (>50 mW) and wideband (>50 nm) 1.3 μm super-luminescent diodes," Electron. Lett. **41**(8), 500–501 (2005).
10. Z. C. Wang, P. Jin, X. Q. Lv, X. K. Li, and Z. G. Wang, "High-power quantum dot superluminescent diode with integrated optical amplifier section," Electron. Lett. **47**(21), 1191–1193 (2011).
11. X. Li, P. Jin, Q. An, Z. Wang, X. Lv, H. Wei, J. Wu, J. Wu, and Z. Wang, "Experimental investigation of wavelength-selective optical feedback for a high-power quantum dot superluminescent device with two-section structure," Opt. Express **20**(11), 11936–11943 (2012).
12. X. Li, P. Jin, Q. An, Z. Wang, X. Lv, H. Wei, J. Wu, J. Wu, and Z. Wang, "A high-performance quantum dot superluminescent diode with a two-section structure," Nanoscale Res. Lett. **6**(1), 625 (2011).
13. X. Li, P. Jin, Q. An, Z. Wang, X. Lv, H. Wei, J. Wu, J. Wu, and Z. Wang, "Improved continuous-wave performance of two-tection quantum-dot superluminescent diodes by using epi-down mounting process," IEEE Photonics Technol. Lett. **24**(14), 1188–1190 (2012).
14. H. Huang and D. G. Deppe, "Rate equation model for nonequilibrium operating conditions in a self-organized quantum-dot laser," IEEE J. Quantum Electron. **37**(5), 691–698 (2001).
15. P. Bardella, M. Rossetti, and I. Montrosset, "Modeling of broadband chirped quantum-dot super-luminescent diodes," IEEE J. Sel. Top. Quantum Electron. **15**(3), 785–791 (2009).
16. M. Tsuda, T. Inoue, T. Kita, and O. Wada, "Broadband light sources using InAs quantum dots with InGaAs strain-reducing layers," Phys. Status Solidi **8**(2), 331–333 (2011).
17. S. Haggett, M. Krakowski, I. Montrosset, and M. A. Cataluna, "High-power quantum-dot tapered tunable external-cavity lasers based on chirped and unchirped structures," Opt. Express **22**(19), 22854–22864 (2014).
18. S. E. White and M. A. Cataluna, "Unlocking spectral versatility from broadly–tunable quantum–dot lasers," Photonics **2**(2), 719–744 (2015).
19. B. V. Volovik, A. F. Tsatsul'nikov, D. A. Bedarev, A. Y. Egorov, A. E. Zhukov, A. R. Kovsh, N. N. Ledentsov, M. V. Maksimov, N. A. Maleev, Y. G. Musikhin, A. A. Suvorova, V. M. Ustinov, P. S. Kop'ev, Z. I. Alferov, D. Bimberg, and P. Werner, "Long-wavelength emission in structures with quantum dots formed in the stimulated decomposition of a solid solution at strained islands," Semiconductors **33**(8), 901–905 (1999).

#358589 https://doi.org/10.1364/OE.27.010981
Journal © 2019 Received 25 Jan 2019; revised 22 Mar 2019; accepted 22 Mar 2019; published 4 Apr 2019

Optics EXPRESS

20. T. Xu, P. Bardella, M. Rossetti, and I. Montrosset, "Beam propagation method simulation and analysis of quantum dot flared semiconductor optical amplifiers in continuous wave high-saturation regime," IET Optoelectron. **6**(2), 110–116 (2012).
21. M. Rossetti, P. Bardella, and I. Montrosset, "Numerical investigation of power tunability in two-section QD superluminescent diodes," Opt. Quantum Electron. **40**(14–15), 1129–1134 (2008).
22. E. V. Andreeva, P. I. Lapin, V. V. Prokhorov, and S. D. Yakubovich, "Quantum-dot superluminescent diodes with improved performance," Quantum Electron. **37**(4), 331–333 (2007).
23. E. V. Andreeva, A. E. Zhukov, V. V. Prokhorov, V. M. Ustinov, and S. D. Yakubovich, "Superluminescent InAs/AlGaAs/GaAs quantum dot heterostructure diodes emitting in the 1100–1230-nm spectral range," Quantum Electron. **36**(6), 527–531 (2006).
24. Y. Morishima, J. Yaguchi, A. Mukai, T. Ohgoh, and H. Asano, "Longitudinal bandgap modulated broadband (>150 nm) InGaAs/GaAs MQWs superluminescent diodes by selective area MOVPE growth," Electron. Lett. **45**(10), 521–522 (2009).
25. M. T. Crowley, N. Patel, T. A. Saiz, M. E. Emawy, T. A. Nilsen, N. A. Naderi, S. D. Mukherjee, B. O. Fimland, and L. F. Lester, "Modelling the spectral emission of multi-section quantum dot superluminescent light-emitting diodes," Semicond. Sci. Technol. **27**(6), 065011 (2012).
26. M. H. Park, S. J. Park, J. D. Song, W. J. Choi, K. W. Kim, J. Y. Lim, Y. J. Lee, and J. H. Park, "Growth and spectral analysis of stacked quantum dots for broadband superluminescent diodes," J. Korean Phys. Soc. **62**(4), 595–600 (2013).
27. R. Yao, N. Weir, C.-S. Lee, and W. Guo, "Broadband chirped InAs Quantum-dot superluminescent light-emitting diodes with $In_x Al_{1-x} As$ strain-reducing layers," IEEE Photonics J. **8**(3), 1–7 (2016).
28. H. S. Djie, C. E. Dimas, D.-N. Wang, B.-S. Ooi, J. C. M. Hwang, G. T. Dang, and W. H. Chang, "InGaAs/GaAs Quantum-dot superluminescent diode for optical sensor and imaging," IEEE Sens. J. **7**(2), 251–257 (2007).
29. F. Wang, P. Jin, J. Wu, Y. Wu, F. Hu, and Z. Wang, "Active multi-mode-interferometer broadband superluminescent diodes," J. Semicond. **37**(1), 014006 (2016).
30. M. Rossetti, A. Markus, A. Fiore, L. Occhi, and C. Velez, "Quantum dot superluminescent diodes emitting at 1.3 μm," IEEE Photonics Technol. Lett. **17**(3), 540–542 (2005).
31. S. Hartmann and W. Elsäßer, "A novel semiconductor-based, fully incoherent amplified spontaneous emission light source for ghost imaging," Sci. Rep. **7**(1), 41866 (2017).
32. Q. Jiang, M. Tang, S. Chen, J. Wu, A. Seeds, and H. Liu, "InAs/GaAs quantum-dot superluminescent diodes monolithically grown on a Ge substrate," Opt. Express **22**(19), 23242–23248 (2014).
33. Z. Y. Zhang, I. J. Luxmoore, Q. Jiang, H. Y. Liu, K. M. Groom, D. T. Childs, M. Hopkinson, A. G. Cullis, and R. A. Hogg, "Broadband quantum dot superluminescent LED with angled facet formed by focused ion beam etching," Electron. Lett. **43**(10), 587–589 (2007).
34. N. Krstajić, L. E. Smith, S. J. Matcher, D. T. D. Childs, M. Bonesi, P. D. L. Greenwood, M. Hugues, K. Kennedy, M. Hopkinson, K. M. Groom, S. MacNeil, R. A. Hogg, and R. Smallwood, "Quantum dot superluminescent diodes for optical coherence tomography: skin imaging," IEEE J. Sel. Top. Quantum Electron. **16**(4), 748–754 (2010).
35. M. Blazek, W. Elsässer, M. Hopkinson, P. Resneau, M. Krakowski, M. Rossetti, P. Bardella, M. Gioannini, and I. Montrosset, "Coherence function control of Quantum Dot Superluminescent Light Emitting Diodes by frequency selective optical feedback," Opt. Express **17**(16), 13365–13372 (2009).
36. Z. Y. Zhang, Q. Jiang, I. J. Luxmoore, and R. A. Hogg, "A p-type-doped quantum dot superluminescent LED with broadband and flat-topped emission spectra obtained by post-growth intermixing under a GaAs proximity cap," Nanotechnology **20**(5), 055204 (2009).
37. S. K. Ray, K. M. Groom, R. Alexander, K. Kennedy, H. Y. Liu, M. Hopkinson, and R. A. Hogg, "Design, growth, fabrication, and characterization of InAs/GaAs 1.3 μm quantum dot broadband superluminescent light emitting diode," J. Appl. Phys. **100**(10), 103105 (2006).
38. Y. Noguchi, H. Yasaka, and O. Mikami, "Tandem active layer superluminescent diode with a very wide spectrum," Appl. Phys. Lett. **58**(18), 1976–1978 (1991).
39. M. Z. M. Khan, H. H. Alhashim, T. K. Ng, and B. S. Ooi, "High-power and high-efficiency 1.3 μm superluminescent diode with flat-top and ultrawide emission bandwidth," IEEE Photonics J. **7**(1), 1–8 (2015).
40. Y. Qu, H. Li, J. X. Zhang, B. Bo, X. Gao, and G. Liu, "High performance 1.3 μm InGaAsN superluminescent diodes," Sci. China Ser. E Technol. Sci. **52**(8), 2396–2399 (2009).
41. C.-H. Tsai, Y.-S. Su, C.-W. Tsai, D. P. Tsai, and C.-F. Lin, "High-power angled broad-area 1.3-μm laser diodes with good beam quality," IEEE Photonics Technol. Lett. **16**(11), 2412–2414 (2004).
42. M. D. Bayleyegn, H. Makhlouf, C. Crotti, K. Plamann, and A. Dubois, "Ultrahigh resolution spectral-domain optical coherence tomography at 1.3μm using a broadband superluminescent diode light source," Opt. Commun. **285**(24), 5564–5569 (2012).
43. J. Wang, M. J. Hamp, and D. T. Cassidy, "Design considerations for asymmetric multiple quantum well broad spectral width superluminescent diodes," IEEE J. Quantum Electron. **44**(12), 1256–1262 (2008).
44. Y. C. Xin, A. Martinez, T. Saiz, A. J. Moscho, Y. Li, T. A. Nilsen, A. L. Gray, and L. F. Lester, "1.3-μm quantum-dot multisection superluminescent diodes with extremely broad bandwidth," IEEE Photonics Technol. Lett. **19**(7), 501–503 (2007).
45. M. Sugo, R. Yoshimura, and Y. Shibata, "High-power (>80 mW) and high-efficiency (>30%) 1.3 μm super-luminescent diodes," Electron. Lett. **42**(21), 1245–1246 (2006).

#358589 https://doi.org/10.1364/OE.27.010981
Journal © 2019 Received 25 Jan 2019; revised 22 Mar 2019; accepted 22 Mar 2019; published 4 Apr 2019

Optics EXPRESS

46. Y. C. Yoo, I. K. Han, and J. H. Kim, "High-power InAs quantum-dot superluminescent diodes with offset J-shaped waveguides," J. Korean Phys. Soc. **61**(8), 1325–1327 (2012).
47. S. Haffouz, M. Rodermans, P. J. Barrios, J. Lapointe, S. Raymond, Z. Lu, and D. Poitras, "Broadband superluminescent diodes with height-engineered InAs-GaAs quantum dots," Electron. Lett. **46**(16), 1144–1146 (2010).
48. I. Tsubaki, Y. Harada, and T. Kita, "High-resolution optical coherence tomography using broadband light source with strain-controlled InAs/GaAs quantum dots," Phys. Status Solidi **9**(12), 2473–2476 (2012).
49. N. Ozaki, D. T. D. Childs, J. Sarma, T. S. Roberts, T. Yasuda, H. Shibata, H. Ohsato, E. Watanabe, N. Ikeda, Y. Sugimoto, and R. A. Hogg, "Superluminescent diode with a broadband gain based on self-assembled InAs quantum dots and segmented contacts for an optical coherence tomography light source," J. Appl. Phys. **119**(8), 083107 (2016).
50. Y. Zhou, J. Zhang, Y. Ning, Y. Zeng, J. Zhang, X. Zhang, L. Qin, and L. Wang, "Bimodal-sized quantum dots for broad spectral bandwidth emitter," Opt. Express **23**(25), 32230–32237 (2015).
51. H. Fa-Jie, J. Peng, W. Yan-Hua, W. Fei-Fei, W. Heng, W. Zhan-Guo, "Broadband and high-speed swept external-cavity laser using a quantum-dot superluminescent diode as gain device," Chin. Phys. B **24**(10), 104212 (2015).
52. G. Du, G. Devane, K. A. Stair, S. Wu, R. P. H. Chang, Y. Zhao, Z. Sun, Y. Liu, X. Jiang, and W. Han, "The monolithic integration of a superluminescent diode with a power amplifier," IEEE Photonics Technol. Lett. **10**(1), 57–59 (1998).
53. P. A. Evans, P. Blood, and J. S. Roberts, "Carrier distribution in quantum well lasers," Semicond. Sci. Technol. **9**(9), 1740–1743 (1994).
54. T. C. Newell, M. W. Wright, H. Hou, and L. F. Lester, "Carrier distribution, spontaneous emission and gain engineering in lasers with nonidentical quantum wells," IEEE J. Sel. Top. Quantum Electron. **5**(3), 620–626 (1999).
55. M. Rossetti, P. Bardella, M. Gioannini, and I. Montrosset, "Carrier transport effects in multi layer quantum dot lasers and SLDs," in *ECIO'08 Eindhoven - Proceedings of the 14th European Conference on Integrated Optics and Technical Exhibition, Contributed and Invited Papers* (European Conference on Integrated Photonics, 2008).
56. X. Q. Lv, N. Liu, P. Jin, and Z. G. Wang, "Broadband emitting superluminescent diodes with InAs quantum dots in AlGaAs Matrix," IEEE Photonics Technol. Lett. **20**(20), 1742–1744 (2008).

#358589 https://doi.org/10.1364/OE.27.010981
Journal © 2019 Received 25 Jan 2019; revised 22 Mar 2019; accepted 22 Mar 2019; published 4 Apr 2019